

DTIC FILE COPY

AEROSPACE REPORT NO.
TOR-0090(5470-01)-3

④

Photochemical Spacecraft Self-Contamination: Laboratory Results and Systems Impacts

Prepared by

T. B. STEWART, G. S. ARNOLD, D. F. HALL, D. C. MARVIN,
W. C. HWANG, R. C. YOUNG OWL, and H. D. MARTEN
Chemistry and Physics Laboratory
Laboratory Operations

25 July 1990

Prepared for

SPACE SYSTEMS DIVISION
AIR FORCE SYSTEMS COMMAND
Los Angeles Air Force Base
P. O. Box 92960
Los Angeles, CA 90009-2960

Contract No. F04701-88-C-0089



Laboratory Operations

THE AEROSPACE CORPORATION

APPROVED FOR PUBLIC RELEASE;
DISTRIBUTION UNLIMITED

AD-A226 488

005

LABORATORY OPERATIONS

The Aerospace Corporation functions as an "architect-engineer" for national security projects, specializing in advanced military space systems. Providing research support, the corporation's Laboratory Operations conducts experimental and theoretical investigations that focus on the application of scientific and technical advances to such systems. Vital to the success of these investigations is the technical staff's wide-ranging expertise and its ability to stay current with new developments. This expertise is enhanced by a research program aimed at dealing with the many problems associated with rapidly evolving space systems. Contributing their capabilities to the research effort are these individual laboratories:

Aerophysics Laboratory: Launch vehicle and reentry fluid mechanics, heat transfer and flight dynamics; chemical and electric propulsion, propellant chemistry, chemical dynamics, environmental chemistry, trace detection; spacecraft structural mechanics, contamination, thermal and structural control; high temperature thermomechanics, gas kinetics and radiation; cw and pulsed chemical and excimer laser development, including chemical kinetics, spectroscopy, optical resonators, beam control, atmospheric propagation, laser effects and countermeasures.

Chemistry and Physics Laboratory: Atmospheric chemical reactions, atmospheric optics, light scattering, state-specific chemical reactions and radiative signatures of missile plumes, sensor out-of-field-of-view rejection, applied laser spectroscopy, laser chemistry, laser optoelectronics, solar cell physics, battery electrochemistry, space vacuum and radiation effects on materials, lubrication and surface phenomena, thermionic emission, photosensitive materials and detectors, atomic frequency standards, and environmental chemistry.

Electronics Research Laboratory: Microelectronics, solid-state device physics, compound semiconductors, radiation hardening; electro-optics, quantum electronics, solid-state lasers, optical propagation and communications; microwave semiconductor devices, microwave/millimeter wave measurements, diagnostics and radiometry, microwave/millimeter wave thermionic devices; atomic time and frequency standards; antennas, rf systems, electromagnetic propagation phenomena, space communication systems.

Materials Sciences Laboratory: Development of new materials: metals, alloys, ceramics, polymers and their composites, and new forms of carbon; nondestructive evaluation, component failure analysis and reliability; fracture mechanics and stress corrosion; analysis and evaluation of materials at cryogenic and elevated temperatures as well as in space and enemy-induced environments.

Space Sciences Laboratory: Magnetospheric, auroral and cosmic ray physics, wave-particle interactions, magnetospheric plasma waves; atmospheric and ionospheric physics, density and composition of the upper atmosphere, remote sensing using atmospheric radiation; solar physics, infrared astronomy, infrared signature analysis; effects of solar activity, magnetic storms and nuclear explosions on the earth's atmosphere, ionosphere and magnetosphere; effects of electromagnetic and particulate radiations on space systems; space instrumentation.

UNCLASSIFIED

SECURITY CLASSIFICATION OF THIS PAGE

REPORT DOCUMENTATION PAGE				
1a. REPORT SECURITY CLASSIFICATION Unclassified		1b. RESTRICTIVE MARKINGS		
2a. SECURITY CLASSIFICATION AUTHORITY		3. DISTRIBUTION/AVAILABILITY OF REPORT Approved for public release; distribution unlimited.		
2b. DECLASSIFICATION/DOWNGRADING SCHEDULE				
4. PERFORMING ORGANIZATION REPORT NUMBER(S) TOR-0090(5470-01)-3		5. MONITORING ORGANIZATION REPORT NUMBER(S)		
6a. NAME OF PERFORMING ORGANIZATION The Aerospace Corporation Laboratory Operations	6b. OFFICE SYMBOL (if applicable)	7a. NAME OF MONITORING ORGANIZATION Space Systems Division		
6c. ADDRESS (City, State, and ZIP Code) El Segundo, CA 90245-4691		7b. ADDRESS (City, State, and ZIP Code) Los Angeles Air Force Base Los Angeles, CA 90009-2960		
8a. NAME OF FUNDING/SPONSORING ORGANIZATION	8b. OFFICE SYMBOL (if applicable)	9. PROCUREMENT INSTRUMENT IDENTIFICATION NUMBER F04701-88-C-0089		
8c. ADDRESS (City, State, and ZIP Code)		10. SOURCE OF FUNDING NUMBERS		
		PROGRAM ELEMENT NO.	PROJECT NO.	TASK NO.
		WORK UNIT ACCESSION NO.		
11. TITLE (Include Security Classification) Photochemical Spacecraft Self-Contamination: Laboratory Results and Systems Impacts				
12. PERSONAL AUTHOR(S) Stewart, Thomas B., Arnold, Graham S., Hall, David F., Marvin, Dean C., Hwang, Warren C., Young Owl, Rolaine C., and Marten, H. Daniel				
13a. TYPE OF REPORT	13b. TIME COVERED FROM _____ TO _____	14. DATE OF REPORT (Year, Month, Day) 1990 July 25	15. PAGE COUNT 42	
16. SUPPLEMENTARY NOTATION.				
17. COSATI CODES		18. SUBJECT TERMS (Continue on reverse if necessary and identify by block number)		
FIELD	GROUP	SUB-GROUP		
		-VUV Radiation Contamination		
		Organic Films		
19. ABSTRACT (Continue on reverse if necessary and identify by block number)				
<p>It has become clear that photochemical reactions induced by solar vacuum ultraviolet (VUV) radiation play a substantial role in contaminant accretion and effects. A series of laboratory measurements of the absolute rates of adsorption, desorption, and VUV-induced deposition of contaminants have been made under simulated spacecraft conditions. The results of these experiments, together with analyses of operational and experimental flight data, show conclusively that the role of sunlight is not merely to darken or fix previously condensed contaminant films, but also to promote the irreversible deposition of contaminant films under conditions in which condensation would not occur. A simple model of the kinetics of photochemical deposition, based on a competition between desorption and photolysis of a transiently adsorbed contaminant molecule, using experimentally measured parameters, is reasonably successful in describing the deposition process. These laboratory experiments and analyses of space-flight experience reveal that photochemical deposition is a significant mechanism whereby contaminant films accrete on orbit and must be considered in the design of future vehicles. (J5)</p>				
20. DISTRIBUTION/AVAILABILITY OF ABSTRACT		21. ABSTRACT SECURITY CLASSIFICATION		
<input checked="" type="checkbox"/> UNCLASSIFIED/UNLIMITED <input type="checkbox"/> SAME AS RPT. <input type="checkbox"/> DTIC USERS		Unclassified		
22a. NAME OF RESPONSIBLE INDIVIDUAL		22b. TELEPHONE (Include Area Code)	22c. OFFICE SYMBOL	

**PHOTOCHEMICAL SPACECRAFT SELF-CONTAMINATION:
LABORATORY RESULTS AND SYSTEMS IMPACTS**

Prepared by

T. B. Stewart, G. S. Arnold, D. F. Hall, D. C. Marvin,
W. C. Hwang, R. C. Young Owl, and H. D. Marten
Chemistry and Physics Laboratory

25 July 1990



Laboratory Operations
THE AEROSPACE CORPORATION
El Segundo, CA 90245-4691

Prepared for

SPACE SYSTEMS DIVISION
AIR FORCE SYSTEMS COMMAND
Los Angeles Air Force Base
P. O. Box 92960
Los Angeles, CA 90009-2960

Contract No. F04701-88-C-0089

Accession For	
NTIS GASI	<input checked="" type="checkbox"/>
DTIC TAB	<input type="checkbox"/>
Unannounced	<input type="checkbox"/>
Justification	
By	
Distribution/	
Availability Codes	
Dist	Avail and/or Special
A-1	




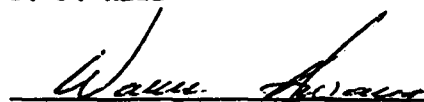
APPROVED FOR PUBLIC RELEASE;
DISTRIBUTION UNLIMITED

PHOTOCHEMICAL SPACECRAFT SELF-CONTAMINATION:
LABORATORY RESULTS AND SYSTEMS IMPACTS

Prepared by


T. B. Stewart

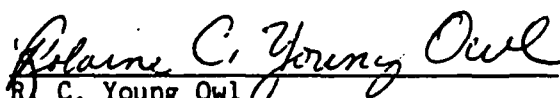

D. F. Hall


W. C. Hwang



H. D. Marten

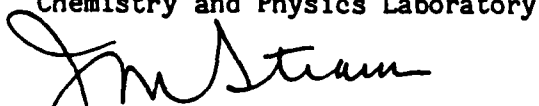

G. S. Arnold

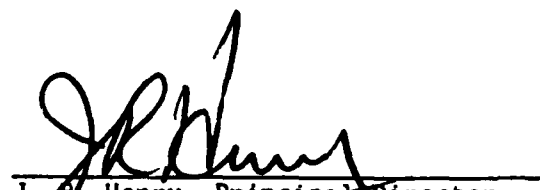

D. C. Marvin


R. C. Young Owl

Approved by


H. K. A. Kan, Head
Surface Science Department
Chemistry and Physics Laboratory


J. M. Straus, Director
Chemistry and Physics Laboratory
Laboratory Operations


J. P. Henry, Principal Director
Navigation Satellite Systems
Directorate
Space Program Operations
Programs Group

The information in a Technical Operating Report is developed for a particular program and is therefore not necessarily of broader technical applicability.

ACKNOWLEDGMENTS

It is a pleasure to acknowledge the contributions of J. H. Hecht, L. J. Ortega, and E. R. Schnauss in the initiation of the experimental program, and of A. R. Calloway in the design and fabrication of the VUV resonance lamps. The authors further express their gratitude to R. R. Hayes and E. A. Zeiner for many useful discussions during the course of this work and to H. K. A. Kan for technical guidance. We further thank W. Muroch for many useful discussions about the performance and configuration of the GPS vehicle, and W. Pence for supplying his unpublished data.

CONTENTS

NOMENCLATURE.....	xi
I. INTRODUCTION.....	1
II. LABORATORY EXPERIMENTS.....	7
A. Experimental.....	7
B. Results.....	9
III. APPLICATION TO SATELLITE PERFORMANCE.....	19
A. SDS Radiator.....	19
B. GPS Solar Array Degradation.....	20
IV. CONCLUSION.....	29
REFERENCES.....	31

FIGURES

1.	Increase in Solar Absorptance of Fused Silica Second Surface Silver Mirrors on Several Satellites.....	2
2.	Predicted and Measured Power Production Capability for the Solar Arrays on Five GPS Block I Vehicles.....	3
3.	Plot of the Reciprocal of the DC-704 Isothermal Photochemical Deposition Efficiency on a Platinum Substrate vs the Incident Flux (at 306 K).....	10
4.	Plot of the Reciprocal of the DEHP Isothermal Photochemical Deposition Efficiency on a Platinum Substrate vs the Incident Flux (at 303 K).....	10
5.	Arrhenius Plot of DC-704 Photochemical Deposition Rate at Constant Incident Flux vs Reciprocal Substrate Temperature from Two Experiments.....	11
6.	Arrhenius Plot (in Substrate Temperature) of the DEHP Photochemical Deposition Rate at Constant Incident Flux.....	11
7.	Condensation and Thermal Desorption of Outgassing Products from Kevlar/Epoxy in the Absence of VUV Illumination (Blank Run).....	16
8.	Condensation and Thermal Desorption of Outgassing Products from Kevlar/Epoxy in the Presence of VUV Illumination (Irradiated Run).....	16
9.	Percent of Deposited Mass of Kevlar/Epoxy Outgassing Products Remaining on the TQCM Surface as a Function of Substrate Temperature Showing Increased Retention of VUV-Irradiated TQCM.....	17
10.	Percent of Deposited Mass of DEHP Remaining on the TQCM surface as a Function of Substrate Temperature.....	17
11.	Compilation of Photochemical Deposition of Rate Data for DC-704, DEHP, and a Contaminant Mixture Used by Hayes, for Several Substrate Temperatures and Identities, Compared to the Estimated Environment of the SDS Radiator.....	21
12.	Predicted and Measured Power Production Capability of NAVSTAR-4 Solar Arrays.....	23

FIGURES (Continued)

13.	Simplified Model of the GPS Block I Vehicle Used to Estimate the Contaminant Flux Incident on the Solar Array.....	25
14.	Estimate of the Increase in Solar Absorptance of a Fused Silica Mirror Mounted on the GPS Solar Array Compared to the NAVSTAR-5 Calorimeter Data.....	28

TABLES

1.	Arrhenius Parameters for Thermal Desorption of DCO-704 and DEHP from Quartz Crystal Microbalance Surfaces.....	12
2.	Substrate Effect on the Photochemical Deposition of DC-704.....	13
3.	Photochemical Fixing of Kevlar/Epoxy Outgassing Films.....	18
4.	High-Temperature Outgassing of Coated and Bare Kevlar/Epoxy.....	18
5.	Quantities Used in the GPS Solar Array Contamination Model.....	26
6.	Photochemical Deposition Kinetic Parameters.....	27

NOMENCLATURE

A	= prefactor of the Arrhenius expression for a thermal desorption rate coefficient
a_i	= coefficient of photochemical deposition efficiency ($i=1,2$) [See Eq. (7)]
B	= photochemically deposited contaminant molecule or its surface concentration
C	= contaminant precursor molecule
C_s	= adsorbed contaminant precursor molecule or its surface concentration
C_s^*	= photoexcited, adsorbed contaminant precursor molecule or its surface concentration
dA	= differential element of area of a contaminant collector surface
$E(\lambda)$	= spectral response of a silicon solar cell
E_a	= activation energy for the thermal desorption rate coefficient, k_2
e	= contamination deposition efficiency (deposition rate divided by arrival rate)
$f(t)$	= time dependent factor for correcting the silicon cell degradation model for the effects of a darkened contaminant film
$F(x,y)$	= spatial distribution of the flux of contaminant incident on the GPS solar array
F_c	= flux (arrival rate) of contaminant precursor molecules in $\text{cm}^{-2} \text{sec}^{-1}$
$\langle F_s \rangle$	= average rate of deposition of contaminant molecules originating from outgassing from surfaces in the field of view of a collector surface
$\langle F_v \rangle$	= average rate of deposition of contaminant molecules originating from within the vehicle (vented) within the field of view of a collector surface
$h\nu$	= a photon
I_0	= intensity of illumination in photons $\text{cm}^{-2} \text{sec}^{-1}$
$I_s(\lambda)$	= air-mass-zero solar spectrum
k_1	= rate coefficient for adsorption of a contaminant precursor molecule onto a vacant site in $\text{cm}^2 \text{sec}^{-1}$
k_2	= rate coefficient for thermal desorption of an adsorbed molecule in sec^{-1}
k_3	= rate coefficient for photoexcitation of an adsorbed molecule in units of area

k_4	= rate coefficient for the reaction of an excited adsorbed contaminant molecule to form a photochemically fixed contaminant molecule in sec^{-1}
k_5	= rate coefficient for non-reactive decay of an excited adsorbed contaminant molecule in sec^{-1}
P_0	= probability that a contaminant precursor molecule which strikes an unoccupied surface site will stick
q	= quantum yield for photodeposition, $k_4/(k_4+k_5)$
r	= distance between a contaminant source and collector
R	= ideal gas constant
S	= unoccupied surface site, or the concentration of unoccupied sites
S_0	= total concentration of available sites on the surface, in cm^{-2}
T	= temperature in kelvin
t	= time
V_r	= fraction of the total vehicle vent area in the field of view of a contaminant collector surface
x	= contaminant film thickness
α	= solar absorptance
$\Delta\alpha$	= change in solar absorptance
Δm	= total mass outgassed by the GPS vehicle over its orbital life
$\epsilon(\lambda)$	= absorption coefficient of a contaminant film
θ	= angle between the collector surface normal and a vector connecting a contaminant source surface and a collector
λ	= wavelength of light
ρ	= contaminant film density
τ	= time constant for GPS spacecraft outgassing
ϕ	= angle between the source surface normal and a vector connecting a contaminant source and a collector surface

1. INTRODUCTION

Self-contamination of sensitive spacecraft surfaces has long been recognized as potentially limiting the performance and even the useful life of spacecraft. There is a growing body of information on the production, transport, deposition, and effects of spacecraft contaminants. However, if the management of contamination is to become a truly quantitative part of spacecraft design, then a greater understanding of the mechanisms and absolute rates of processes which cause spacecraft self-contamination must be gained. One such process is the photochemical deposition of organic films as a result of solar vacuum ultraviolet radiation.

There is, of course, no doubt that the combination of ultraviolet light and large organic molecules can result in the deposition of tenacious films.¹⁻⁵ However, there is a shortage of data on absolute deposition rates, and the dependence of those rates on contaminant flux, substrate temperature, and substrate identity which could be used to estimate the contribution of photochemical deposition to spacecraft self-contamination. A laboratory effort was undertaken to obtain this information. The initial results of this effort were reported in an earlier paper,⁶ along with a review of the data from the SCATHA ML-12 experiment which revealed the potential importance of this phenomenon in geosynchronous orbit.⁷ For a complete bibliography of papers describing the hardware, results, and data analysis for the SCATHA ML-12 Contamination and Thermal Control Coatings experiment, see Ref. 7.

This report provides a brief summary of the further results of this laboratory effort (which is described in greater detail elsewhere⁸) and discusses the application of the understanding gained to three operational satellite contamination problems (two on-orbit, and one anticipated). The three contamination problems are: 1) darkening of the fused silica mirror radiator on the Satellite Data System (SDS) vehicle, 2) anomalous decay of solar array output on Global Positioning Satellite (GPS) Block I vehicles, and 3) possible contamination of sensitive surfaces of payloads during the orbital transfer period of Inertial Upper Stage (IUS) launches. Each of these effects is described in the remainder of this introduction.

The anomalous degradation of the SDS thermal radiator was discussed in Ref. 6. Figure 1 exhibits a series of curves of the increase in solar absorptance of fused silica mirrors on operational and experimental spacecraft. The behavior of the SDS radiator is indicated. It was originally thought that because the radiator was warmer than the major sources of contamination on the spacecraft, it would not suffer from contamination. However, as Fig. 1 indicates, the radiator's temperature (solar absorptance) rose dramatically on orbit. It was hypothesized that the cause of the contamination was photo-deposition of contaminant films, because the surface was sunlit for a significant fraction of time.

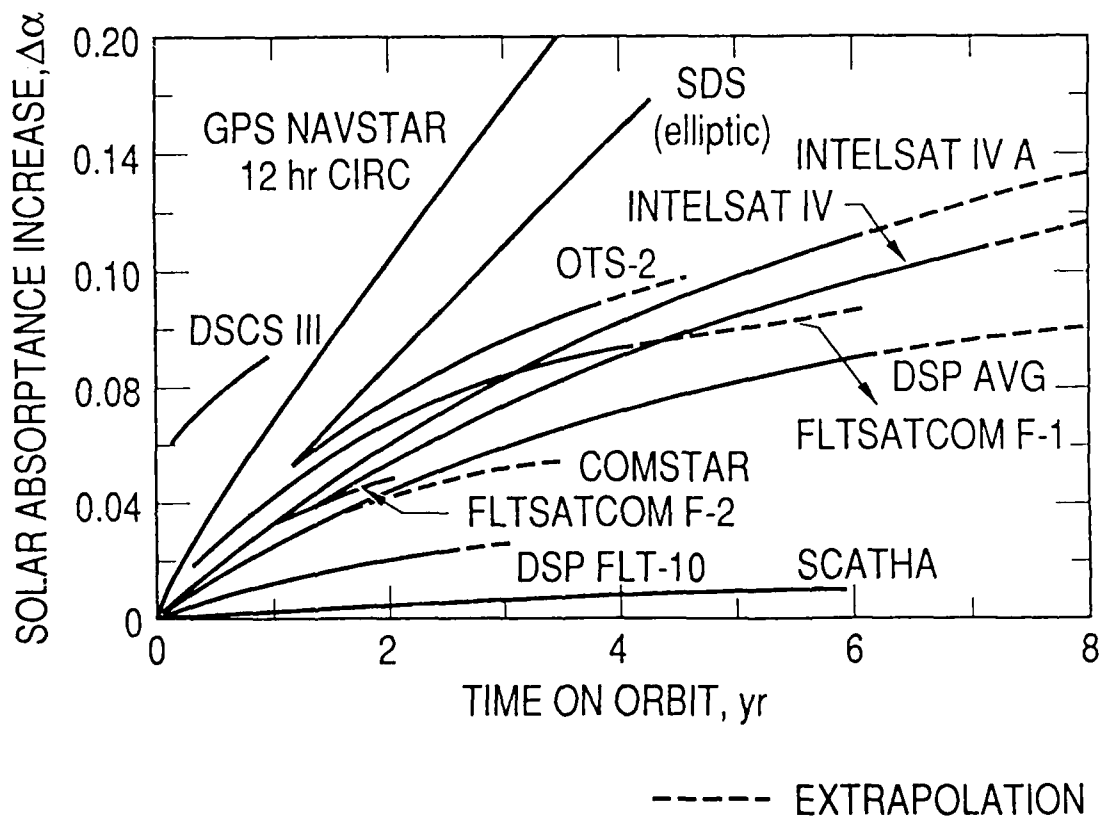


Fig. 1. Increase in Solar Absorptance of Fused Silica Second Surface Silver Mirrors on Several Satellites

The Block I NAVSTAR satellites use silicon solar cells essentially of the K4 1/2 type, which were the state-of-the-art at the time of design. The design life of these spacecraft was five years. The performance of the solar arrays over this period was predicted from the known radiation environments and from data on irradiated cells. The actual solar array output power for five spacecraft estimated from telemetry data is shown in Fig. 2, along with the predicted power based on radiation models. The predicted power for the first five years was supplied by the GPS prime contractor. The extrapolation to 10 years was made by using typical irradiated cell results for the appropriate type cell.⁹ (NAVSTAR-5 did not operate for a sufficiently long time on orbit for the effect being discussed to be manifest.) These data contrast sharply with the prediction, showing essentially linear degradation. The data from all five spacecraft in this group show the same trend. A discrepancy of this magnitude has strong implications for the end of life of the spacecraft and for the design of subsequent generations of GPS and other satellites.

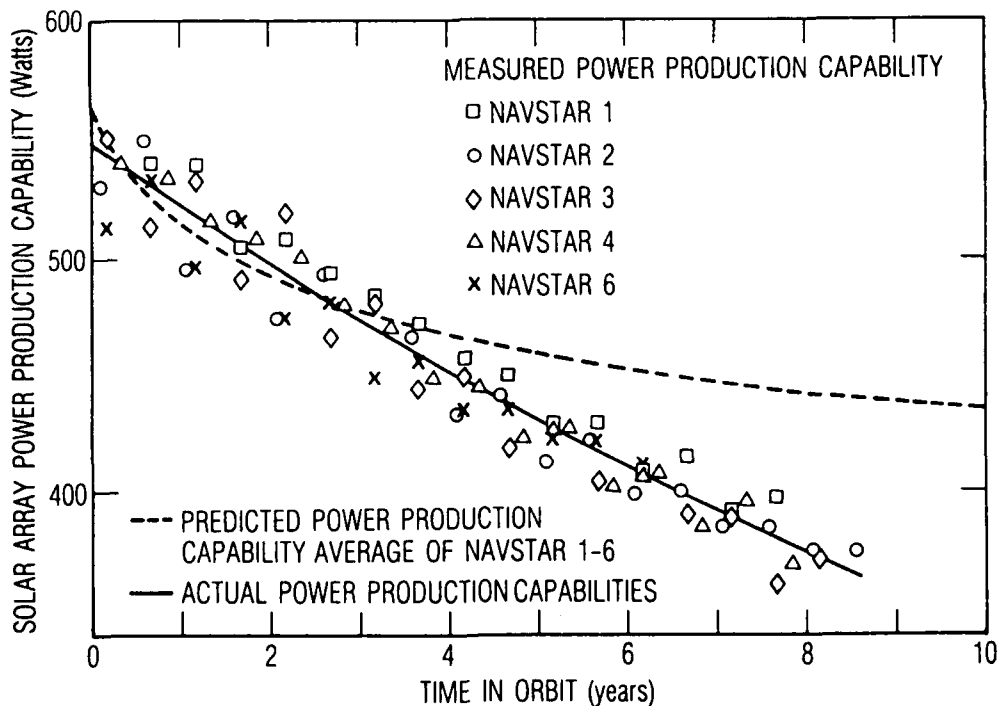


Fig. 2. Predicted and Measured Power Production Capability for the Solar Arrays on Five GPS Block I Vehicles. The prediction includes only the effect of the natural radiation environment on the solar cell performance. The measured capability was inferred from telemetered battery-charging data immediately after eclipse.

Initial attempts to explain the flight data included review of data on radiation-induced degradation of solar cells.⁹ It was found that no silicon solar cells of this type had ever shown linear degradation under irradiation at the anticipated fluences. The possibility of mechanical failure of interconnects, coverglasses, and even cells was considered. Any of these processes would have led to abrupt changes in power output rather than a smooth decrease. These abrupt changes were not observed. Also, it would be unlikely that all five spacecraft in this study would be affected in the identical fashion that has been observed.

The GPS vehicles are three-axis stabilized, with the solar arrays mounted on booms extending from the sides of the main vehicle body. Thus, the solar arrays have a view of the main body, a potential source of contaminants, and are sunlit, which leads one to suspect that they are subject to photochemical contaminant deposition. Furthermore, a fused silica mirror calorimetrically mounted on the solar array of one vehicle, NAVSTAR-5, showed a rapid increase in solar absorptance (see Fig. 1).¹⁰ Thus the possibility of contamination of solar array surfaces on GPS Block I vehicles is quite high. Analyses presented in this report show that photochemical contaminant accretion of the solar cell cover slips is currently the most likely explanation of the anomalous degradation of the GPS solar array output.

After the first solid rocket motor burn (SRM-1) of the IUS booster during the orbital transfer period, heat from the combustion chamber flows outward through the Kevlar®/epoxy motor case, causing its temperature to rise to as high as 265°C. It was anticipated that some of the outgassing products of the heated case would be vented and that it would be possible for sensitive surfaces to have this vent in their fields of view.

In the particular case of the launch of the Defense Support Program (DSP) vehicle, it was realized that solar array surfaces would view the vent. During the outgassing period, the temperatures of these surfaces were expected to be about -50°C. Analytical calculations suggested that 4 $\mu\text{g cm}^{-2}$ of contamination could condense on these surfaces. The concern arose that,

rather than re-evaporating as the surfaces are warmed during a mid-course heat soak period, these molecules would become "fixed" to the surfaces by exposure to the sun's ultraviolet radiation.

In all three cases cited above, it has been hypothesized that it is the action of vacuum ultraviolet (VUV) sunlight which affects the rate of deposition and/or tenacity of the contaminant film. However, it is not the existence of these effects that requires elucidation, but their absolute magnitudes. Section II of this report describes the results of a series of laboratory experiments undertaken to measure the absolute rates of adsorption, desorption, and photochemical deposition of organic contaminant films. (For a more detailed description of the experimental apparatus and results, the reader should consult Ref. 8.) In Section III, the results of these experiments are then related to observed degradation of optical surfaces on the SDS and GPS vehicles.

II. LABORATORY EXPERIMENTS

A. EXPERIMENTAL

Absolute rates of adsorption, desorption, and photochemical deposition were measured in an ultrahigh vacuum system evacuated with a turbomolecular pump and a liquid nitrogen cooled (110 K) shroud to pressures in the range of 2×10^{-9} Torr. The major elements of the test apparatus were a temperature-controlled quartz crystal microbalance (TQCM) for mass detection, a source of contaminant flux (either a Knudsen cell or a thermostatically mounted sample of a nonmetallic spacecraft material), interchangeable vacuum ultraviolet lamps, and a shutter for switching the contaminant "beam" on or off.

Mass accretion was measured with a 5 or 10 MHz doublet quartz crystal microbalance whose mass sensitivities were 1.77×10^{-8} g cm⁻² Hz⁻¹ and 4.42×10^{-9} g cm⁻² Hz⁻¹, respectively. The crystals were mounted to a thermostatically controlled copper block. Long- and short-term fluctuations of the crystal temperature (measured by a copper-constantan thermocouple bonded directly to the crystal face) were the ultimate limit on precision of the measurement. Signal averaging and an empirical correction for the frequency-temperature characteristic of the individual crystals permitted measurement of deposition rates as low as 10^{-9} g cm⁻² hr⁻¹.

Pure substances analogous to those comprising spacecraft contaminants were used in preference to the outgassing flux of spacecraft engineering materials in most of the experiments described in this review. This decision was made to provide better control over contaminant flux and a constant contaminant composition over the course of the experiment. Two molecules were used: tetramethyltetraphenyl-trisiloxane (more commonly known as Dow-Corning 704) and bis(2-ethyl, hexylphthalate) (DEHP, often known by its more generic name, dioctyl phthalate). The flux of contaminant to the detector surface was controlled by adjusting the temperature of the Knudsen cell. (Because pure materials were used for contaminant precursors, the absolute fluxes could be reliably controlled by controlling the temperature of the Knudsen cell. For the vapor pressures of the materials used, see Refs. 11 and 12.)

The radiation sources used were medium-pressure, microwave-excited, rare-gas resonance lamps¹³. The lamps were attached directly to the vacuum system, with the lamp window slightly re-entrant into the chamber. The lamps were filled with either krypton or xenon, providing fluxes of 4.9×10^{12} and 6.9×10^{12} photons $\text{cm}^{-2} \text{sec}^{-1}$, respectively, at wavelengths of 130-190 nm. These photon fluxes are very nearly one sun's intensity in this wavelength range¹⁴

The primary substrates on which adsorption, desorption, and photochemical deposition experiments were performed were the vapor-deposited metal electrodes of the TQCM. Platinum, aluminum, and gold electrodes were used. Witness samples of gold, aluminum, magnesium fluoride, and silicon were also mounted near the TQCM. These samples were used for ex situ spectroscopic analyses of deposited films.

Two types of photodeposition experiments were performed: steady-state deposition and photochemical fixing. In the former, a constant flow of contaminant (analog) was established and the rate of deposition on the VUV-illuminated substrate was measured. Various incident contamination fluxes and substrate temperatures were employed, but in every case the flux was so low that no deposition was detectable when VUV was absent. For details of the experimental procedure, see Ref. 8.

In the second, the outgassing products of the IUS motor case [a layered Kevlar (Kevlar is a registered trade name of E.I. Du Pont de Nemours & Co.) material impregnated with Epon 828 epoxy (Epon 828 is a registered trade name of Shell Chemical Co.)] or DEHP were deposited in the dark on a -55°C TQCM surface. The Kevlar/epoxy samples used were 1-in.-diam \times 1/16-in.-thick coupons cut from a piece of virgin unheated motor casing. The coupon temperature was measured directly with a copper-constantan thermocouple.

The experimental protocol was designed to simulate the temperature histories of the motor casing and the collector surface during the burn and heat-soak period. The casing material was heated to 265°C after a 4 hr conditioning at 100°C to remove water. The contaminant was deposited to a density of $4\text{-}8 \mu\text{g cm}^{-2}$ onto a TQCM maintained at -55°C . Once the desired mass was collected, the source was isolated from the TQCM by closing the shutter,

and the collector surface was warmed to 40°C over a 90 min period. These experiments were performed both in the absence and presence of VUV radiation and were thus "background" and "illuminated." The VUV intensity was approximately equivalent to one sun. Therefore, the experimental conditions constitute a worst case for VUV fixing. A final set of experiments was performed to ascertain whether coating the Kevlar/epoxy material with a conducting paint, Electrodag 447 (Electrodag 447 is a registered trade name of Acheson Products, Inc.), had any effect on the casing's outgassing rate at the high temperatures reached during SRM-1.

B. RESULTS

B.1 STEADY STATE DEPOSITION

The steady state photochemical deposition rate was measured for both contaminant analogs (DC-704 and DEHP) as a function of contaminant flux (arrival rate), surface temperature, and (for DC-704) substrate identity.

Figures 3 and 4 show the dependence of the deposition efficiency on the arrival rate. The data are plotted as the reciprocal of deposition efficiency vs arrival rate. These plots show clearly that the notion of a constant deposition efficiency (sticking coefficient), even at constant surface temperature, is not valid.

Figures 5 and 6 show the temperature dependence of the deposition rate of the two molecules at constant flux. The data are shown as Arrhenius plots in substrate temperature. Note that the deposition rate increases with decreasing temperature. Thus the "activation energy" of the process is negative. Of course, these activation energies are valid only over the range of the measurements (and perhaps to higher temperatures) since extrapolating these plots to lower temperature would eventually lead to a deposition efficiency of greater than 1 (infinite at zero temperature).

The inverse temperature dependence of the photochemical deposition efficiency provides strong support for the hypothesis that photochemical deposition involves photoexcitation of a transiently adsorbed molecule. Thus

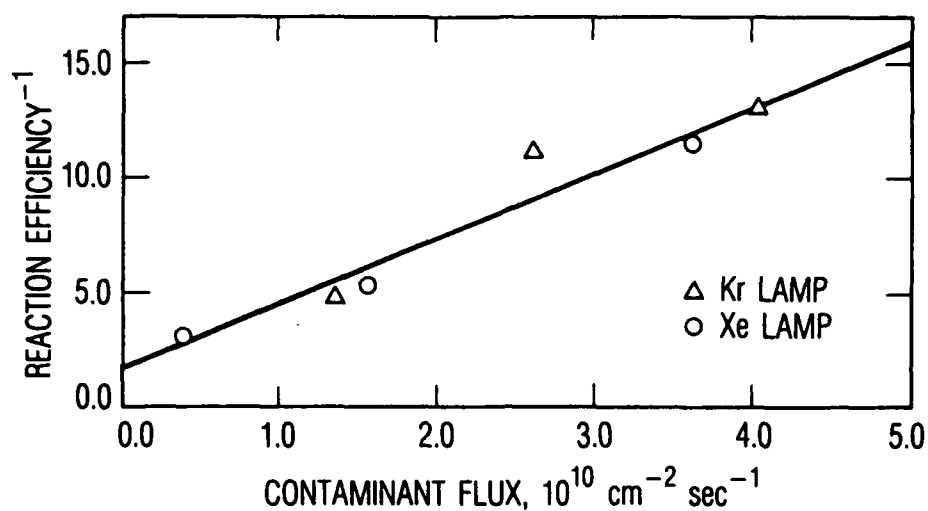


Fig. 3. Plot of the Reciprocal of the DC-704 Isothermal Photochemical Deposition Efficiency on a Platinum Substrate vs the Incident Flux (at 306 K). The solid line is a linear least-squares fit.

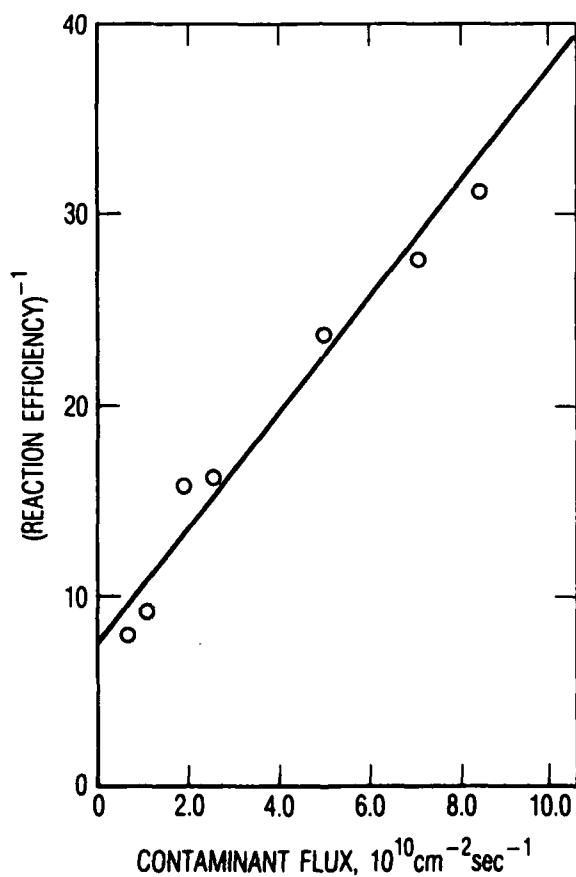


Fig. 4. Plot of the Reciprocal of the DEHP Isothermal Photochemical Deposition Efficiency on a Platinum Substrate vs the Incident Flux (at 303 K). The solid line is a linear least-squares fit.

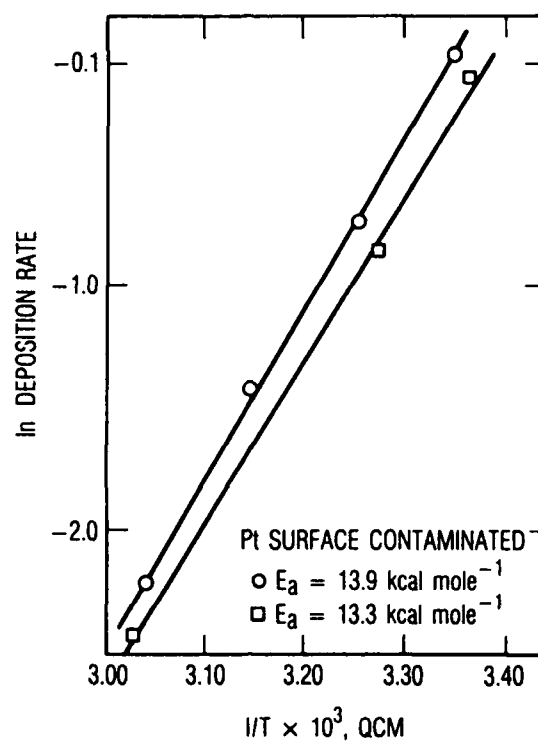


Fig. 5. Arrhenius Plot (in Substrate Temperature) of the DC-704 Photochemical Deposition Rate at Constant Incident Flux vs Reciprocal Substrate Temperature from Two Experiments

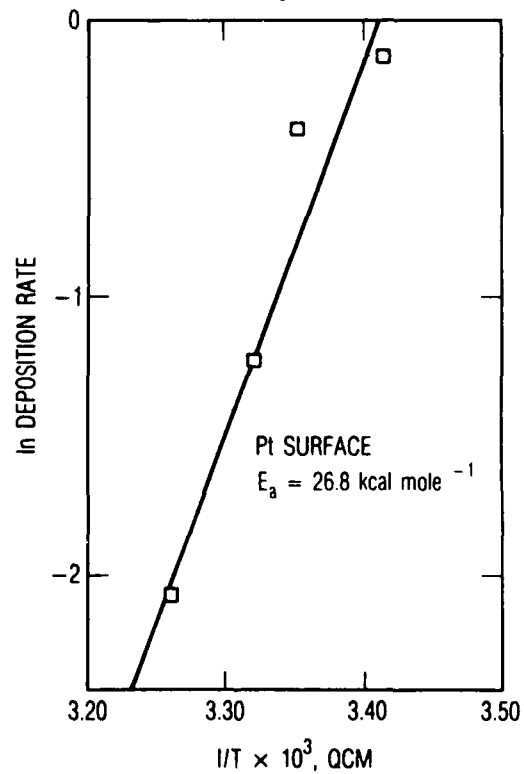


Fig. 6. Arrhenius Plot (in Substrate Temperature) of the DEHP Photochemical Deposition Rate at Constant Incident Flux

an understanding of the residence time, or rate coefficient, for thermal desorption of an adsorbed molecule (in the absence of illumination) is important to understanding the overall deposition process. Measurements of the rate of desorption of DEHP and DC-704 were made from nominally clean TQCM surfaces and from surfaces with photodeposited films (exposed surface). First-order desorption kinetics which exhibited simple Arrhenius behavior were observed. Table 1 shows the Arrhenius parameters for the desorption rate coefficients (k_2) measured.

Table 1. Arrhenius Parameters* for Thermal Desorption of DC-704 and DEHP from Quartz Crystal Microbalance Surfaces

Material	Surface	E_a (kcal mole ⁻¹)	$\ln(A)$ (sec ⁻¹)
DC-704	Al (exposed)	18.4	24.4
DEHP	Pt (exposed)	28.2	41.6
DEHP	Pt (unexposed)	30.8	47.3

*Desorption rate coefficient = $A \exp(-E_a/RT)$

Analysis of the witness samples revealed that deposition was much more rapid on aluminum than on gold. Furthermore, it was clear that deposition occurred on two substrates which were nominally transparent to the illumination: sapphire and magnesium fluoride. The substrate dependence of the deposition rate was dramatically demonstrated by using TQCMs with different electrode materials. Table 2 summarizes these results.

Table 2. Substrate Effect on the Photochemical
Deposition of DC-704*

Sub- strate	Flux (nm/hr)	Temperature (kelvin)	Deposition Rate (nm/hr)	Effi- ciency
Au	0.58	309	0.016	0.027
Au	0.58	304	0.027	0.047
Au	0.64	308	0.027	0.041
Pt	0.44	306	0.096	0.22
Pt	0.44	308	0.084	0.19

*Xenon irradiation.

These experiments were undertaken with the notion that under the conditions of flux and surface temperature of interest, photochemical deposition is a competition between photolysis and desorption of a transiently adsorbed molecule. This kinetic mechanism for the mass accretion by photochemical deposition can be summarized as



where C is the potential contaminant molecule, S is a surface site, and B is a photochemically bound contaminant molecule. The nature of excitation to C^* is not specified. It could include, for example, electronic excitation or radical formation by bond cleavage.

At steady state ($d^2B/dt^2 = 0$), under the assumption of constant total site density ($S + C_s + C_s^* = S_0$), this model predicts an accretion rate of

$$dB/dt \approx \frac{k_3 q I_0 P_0 F_c}{k_2 + k_3 q I_0 + P_0 F_c / S_0} \quad (2)$$

were $q = k_4 / (k_4 + k_5)$.⁸ Examination of Eq. (2) reveals that if the proposed model is valid, then a plot of the reciprocal of the deposition efficiency vs the contaminant flux should be a straight line. The results of the photo-deposition experiments are consistent with this general picture of the deposition process. (see Figs. 3 and 4.)

The slopes and intercepts of the fitted lines in Figs. 3 and 4, combined with the measured values of I_0 , F_c , and k_2 allow one to infer values for the quantities $k_3 q$ and S_0 . The inferred values of $k_3 q$, 8 \AA^2 for DC 704 and $0.4\text{--}1 \text{ \AA}^2$ for DEHP, are very close to the bulk absorption cross sections for these molecules in the vacuum ultraviolet.¹⁵ (The authors are aware of no measurement of the VUV absorption cross section for DEHP; however, the cross section for polystyrene is probably a good value to use as an analog. This molecule's absorption cross section at about 180 nm is 0.5 \AA^2 .)¹⁶ The site densities are on the order of $10^{12}\text{--}10^{13} \text{ cm}^{-2}$, which are reasonable values for monolayer densities for molecules of this size. Furthermore, if one inserts the measured temperature dependence of k_2 into Eq. (1), then the model succeeds in describing the measured temperature dependence of the photochemical deposition rate within about a factor of 2.⁸

A similar model involving substrate excitation could be proposed, but an analysis of these results under such a model indicates that the surface excitation must have an unreasonably long lifetime, hundreds of seconds, and surprisingly small effective VUV absorptivity for the contaminated metal substrate. Furthermore, excitation of the substrate by the VUV radiation

leading to eventual reaction of the contaminant molecule is not considered a probable mechanism based on the photodeposit observed on MgF_2 . MgF_2 is transparent to 130-190 nm radiation, thus precluding any substrate excitation.

Thus, if one accepts the limitations of its several simplifying assumptions, the simple kinetic model clearly can be quite useful in predicting the magnitude of the problem presented by steady-state photochemical contaminant deposition on spacecraft.

B.2 PHOTOCHEMICAL FIXING

Figures 7 and 8 show plots of the QCM frequency (corrected for substrate temperature) vs time for background and irradiated experiments using the Kevlar/epoxy motor casing material, without the conductive coating. Figure 9 shows a plot of the percent mass remaining on the QCM vs the temperature for two such runs. The effect of radiation on the rates of evaporation between the background and irradiated experiments is quite evident.

The results for these two runs are summarized in Table 3. The factor of 2 difference in deposited mass (under nominally identical experimental conditions) reveals the variability in the outgassing rates of the Kevlar/epoxy samples at the high temperatures used in these experiments.

Because the variability of the outgassing rate of the Kevlar/epoxy material produced such a wide range of initial mass densities, a control experiment using DEHP was performed to demonstrate the effect of photochemical fixing during thermal desorption more definitely. Figure 10 shows the results of this experiment.

Table 4 presents the results of a series of experiments performed to ascertain whether an Electrodag conductive coating applied to the motor case would affect its total outgassing rate during the SRM-1 heat-soak period.

Again, the variability in outgassing rate for this engineering material is clear. However, it is also apparent that the conductive coating does not significantly affect the total outgassing rate.

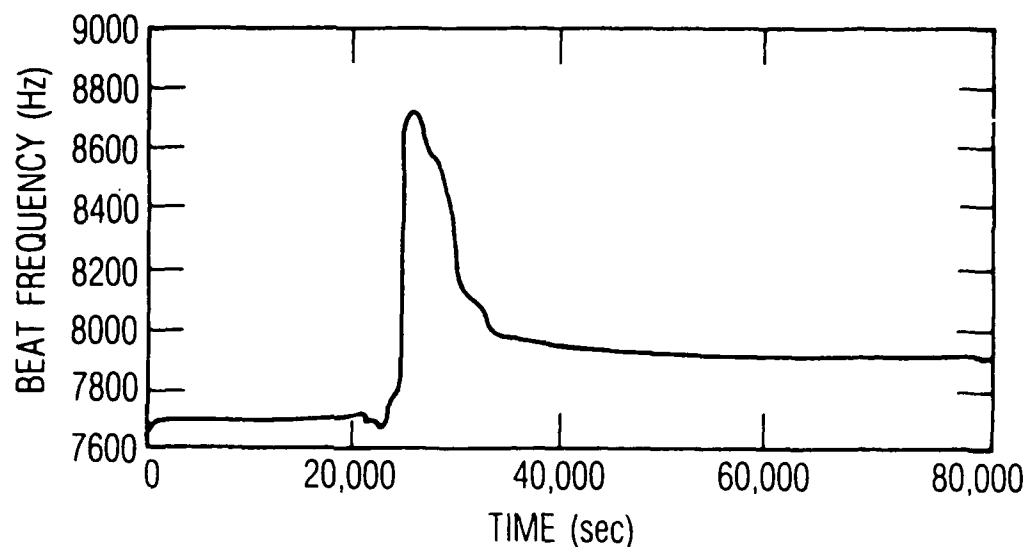


Fig. 7. Condensation and Thermal Desorption of Outgassing Products from Kevlar/Epoxy in the Absence of VUV Illumination (Blank Run)

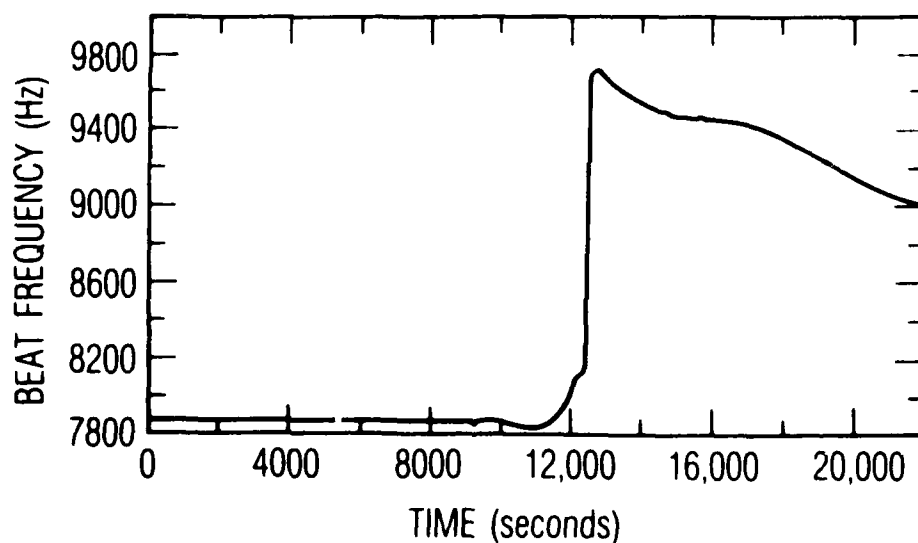


Fig. 8. Condensation and Thermal Desorption of Outgassing Products from Kevlar/Epoxy in the Presence of VUV Illumination (Irradiated Run)

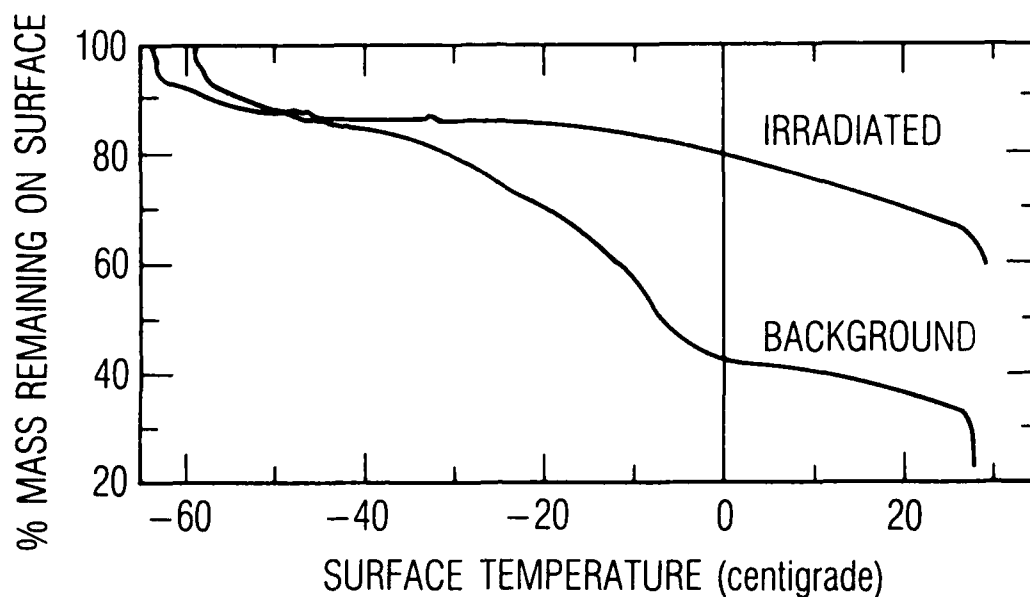


Fig. 9. Percent of Deposited Mass of Kevlar/Epoxy Outgassing Products Remaining on the TQCM Surface as a Function of Substrate Temperature Showing Increased Retention of VUV-Irradidated TQCM

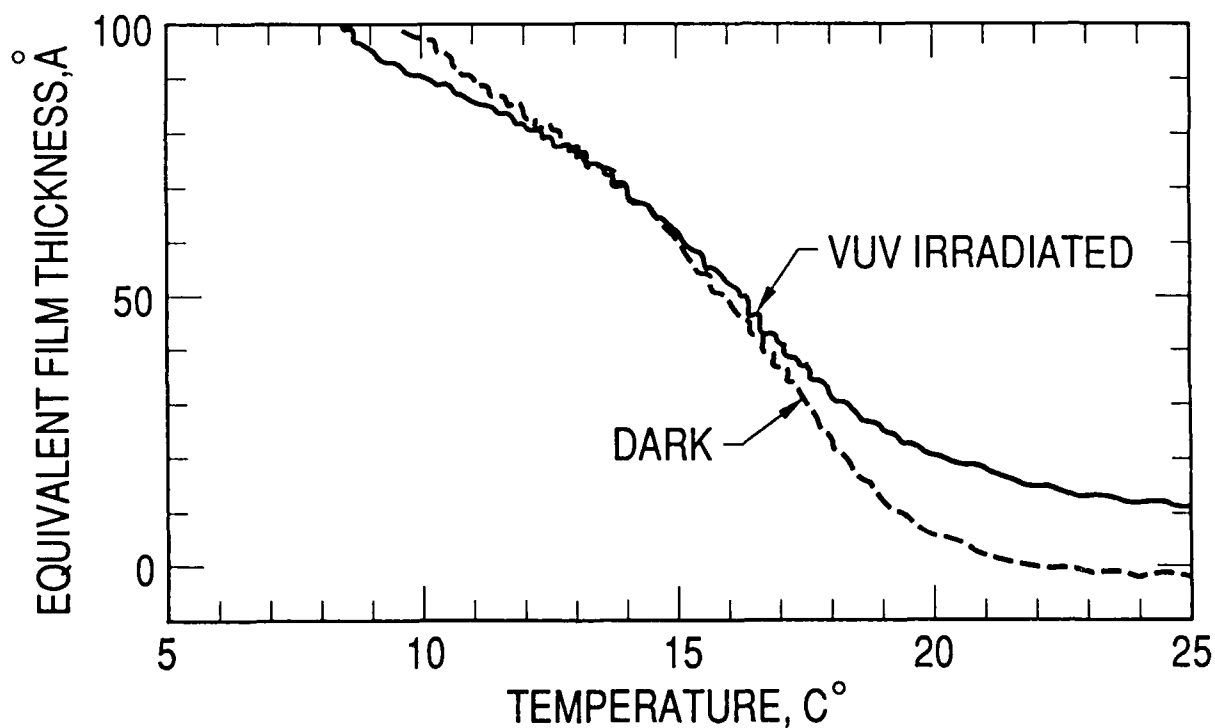


Fig. 10. Percent of Deposited Mass of DEHP Remaining on the TQCM Surface as a Function of Substrate Temperature: Solid Curve, Irradiated Dashed Curve, Background

Table 3. Photochemical Fixing of Kevlar/
Epoxy Outgassing Films

Film Deposited (at -55°C)			Film Remaining (after warming)		
$\mu\text{g cm}^{-2}$	nm*	Xe lamp	$\mu\text{g cm}^{-2}$	nm*	%
4.46	44.6	OFF	0.93	9.3	21
8.27	82.7	ON	4.77	47.7	56

*Assuming film density of 1 g cm^{-3}

Table 4. High Temperature Outgassing of Coated and Bare Kevlar/Epoxy

Sample*	Temperature(°C)		Deposition Rate Total		% Remaining	
	Sample	TQCM	(Å/sec)	($\mu\text{g/cm}^2$)	when 30°C reached	after 48 hrs @ 30°C
Uncoated #1	262	-30	6.5	75		42
Uncoated #2	263	-56	0.65	59	74	37
Coated #1	272	-43	2.5	62	79	37
Coated #2	261	-52	1.1	49	80	55
Coated #3	259	-50	2.1	64	75	37
Coated #4	258	-59	2.3	51	67	40

*The samples designated Coated #1 and #2 were provided by the SRM contractor. The samples designated Coated #3 and #4 were coated in-house following the manufacturer's instructions. They were then baked at 100°C for 10 days in a convection oven to simulate the propellant cure cycle which the rocket motor undergoes after the case is coated.

III. APPLICATION TO SATELLITE PERFORMANCE

This work was originally undertaken to ascertain whether photochemical film deposition could explain the rate of increase in solar absorptance of the SDS satellite radiator. The question at hand was not whether VUV photochemical deposition of large organic molecules occurs, but rather if one could expect the absolute deposition rate to be sufficiently large to account for the observed radiator degradation. Subsequently, the anomalous degradation of the GPS solar array output was revealed. A process of elimination (as usual) led to photochemical contamination's being identified currently as the most likely cause of the unexpected decline in solar array output. Each of these topics is discussed in more detail in this section.

A. SDS RADIATOR

The SDS radiator surface, which was observed to degrade rapidly on orbit, had a direct view of the major vent of the interior of the vehicle. It was estimated⁶ that this vent caused the surfaces in question to experience a total molecular flux of less than $0.4 \mu\text{g cm}^{-2} \text{ hr}^{-1}$, and the relative temperatures of the sources and collectors were such that condensation was not expected to occur. A deposition rate of approximately $1 \text{ ng cm}^{-2} \text{ hr}^{-1}$ was necessary to explain the rate of increase in solar absorptance of the vehicle radiator.

Initial investigations by Hayes⁶ were performed with fluxes of molecules (outgassing from spacecraft engineering materials) much higher than the expected arrival rate. If one extrapolated his results linearly to the appropriate arrival rates, then one would conclude that it was unlikely that photochemical deposition could proceed at a rate necessary to explain the observed spacecraft degradation. However, the background photochemical deposition rate (owing to chamber residual gas) in Hayes's experiment suggested that a linear extrapolation was inappropriate.

The experiments described in section II extended the measurement of absolute deposition rates into the regime of arrival rate expected on orbit. Figure 11 shows a compilation of the results of the steady-state photochemical deposition rate measurements for two different molecules, representative of

spacecraft contaminants, for a range of temperatures and substrates under approximately 1 sun's intensity of vacuum ultraviolet illumination. The box labelled "Elliptical" is bounded by the range of arrival rates expected on the SDS radiator and deposition rates needed to explain the observed increase in solar absorptance. Most of the laboratory rates measured fall within or near these estimated conditions.

Therefore, these laboratory results support the assignment of photochemically deposited contamination as the origin of the unexpectedly high rate of increase in solar absorptance of the SDS fused silica mirror radiator.

B. GPS SOLAR ARRAY DEGRADATION

Since the available radiation degradation models were unable to explain the observed degradation of the GPS solar arrays, analyses were performed to ascertain the likelihood of contamination's being the culprit. The approach used was to show that the amount of the apparent darkening of a fused silica second surface mirror on the NAVSTAR-5 solar array could account for the extra decrease in solar array output, and then to show, on the basis of vehicle configuration and photochemical deposition kinetics, that it was possible to account for the NAVSTAR-5 calorimeter data by contamination.

The curve labeled GPS NAVSTAR in Fig. 1 refers to data taken from a second surface mirror mounted near the center of the solar array of NAVSTAR-5.¹⁰ This sensor was therefore exposed to the same environment as the solar panels. Two methods were used to relate this increase in solar absorptance to decay in solar array power. Both assume that the optical absorbance of such a film will reduce only the array output currents and not affect their voltage capabilities.

The simplest method of computing the cell current reduction is to use the values in Fig. 1 (for GPS) to determine the reduced amount of light reaching the cell. For solar cells the light makes only one pass through the film.

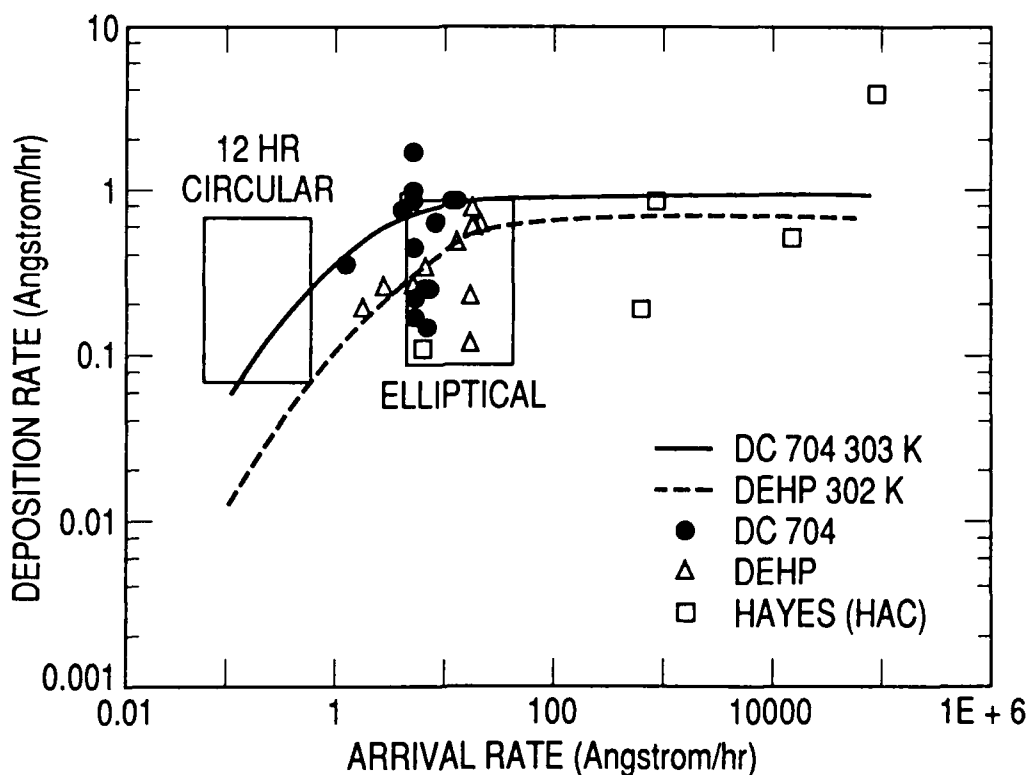


Fig. 11. Compilation of Photochemical Deposition of Rate Data for DC-704, DEHP, and a Contaminant Mixture used by Hayes, for Several Substrate Temperatures and Identities, Compared to the Estimated Environment of the SDS Radiator

Therefore, the attenuation derived from the calorimeter must be divided by two. Under this model the solar array output current is reduced by the factor

$$f(t) = [1 - \alpha_s(t)/2] \quad (3)$$

where t is the time on orbit. The values in the figure have been linearly extrapolated, while bearing in mind that α_s cannot exceed unity.

This approach did, indeed, provide a correction to the radiation damage model that produced good agreement with the observed solar array performance data. Thus, whatever the mechanism for darkening of the NAVSTAR-5 calorimeter might be, it can account for the anomalous decrease in solar array power. However, in using this technique, one makes the not necessarily warranted assumption that the efficiency with which the solar cell converts the air mass zero (AMO) solar spectrum into electric current has the same wavelength

and converts them into heat. This is certainly an approximation, since all of the photon energy can be converted into heat by the absorption process, whereas even ideal solar cells cannot extract greater than the bandgap energy from any photon.

The calculation can be improved by making use of a canonical contaminant film optical absorption spectrum, which, combined with the observed increase in solar absorptance, can be used to compute time-dependent contaminant thickness. The contaminant spectrum may then be convolved over a silicon solar cell response curve¹⁷ to produce a time-dependent decrease in power owing to contaminant absorption. Stated algebraically, the factor by which solar array power is reduced is

$$f(t) = \frac{\int E(\lambda) I_s(\lambda) \exp[-\epsilon(\lambda)x(t)] d\lambda}{\int E(\lambda) I_s(\lambda) d\lambda} \quad (4)$$

The contaminant spectrum, $\epsilon(\lambda)$, was taken from Ref. 18. Zeiner has computed the increase in solar absorptance of a fused silica mirror as a function of thickness for this spectrum.¹⁸ Thus, the only assumption in this calculation is that the shape of this canonical spectrum is a good approximation to that of the films which might accrete on GPS solar array surfaces.

Figure 12 shows the power system output for NAVSTAR-4 (squares), the original radiation-induced degradation predictions (solid line), and a new prediction based on the product of this original model and the more accurate $f(t)$ term just evaluated. The shape of the flight data curve is better represented by the combined effects.

Therefore, one is led to the position that the same mechanism is probably responsible for the degradation of the NAVSTAR-5 calorimeter and the GPS Block I solar arrays. In their original report of the NAVSTAR-5 data, Pence and

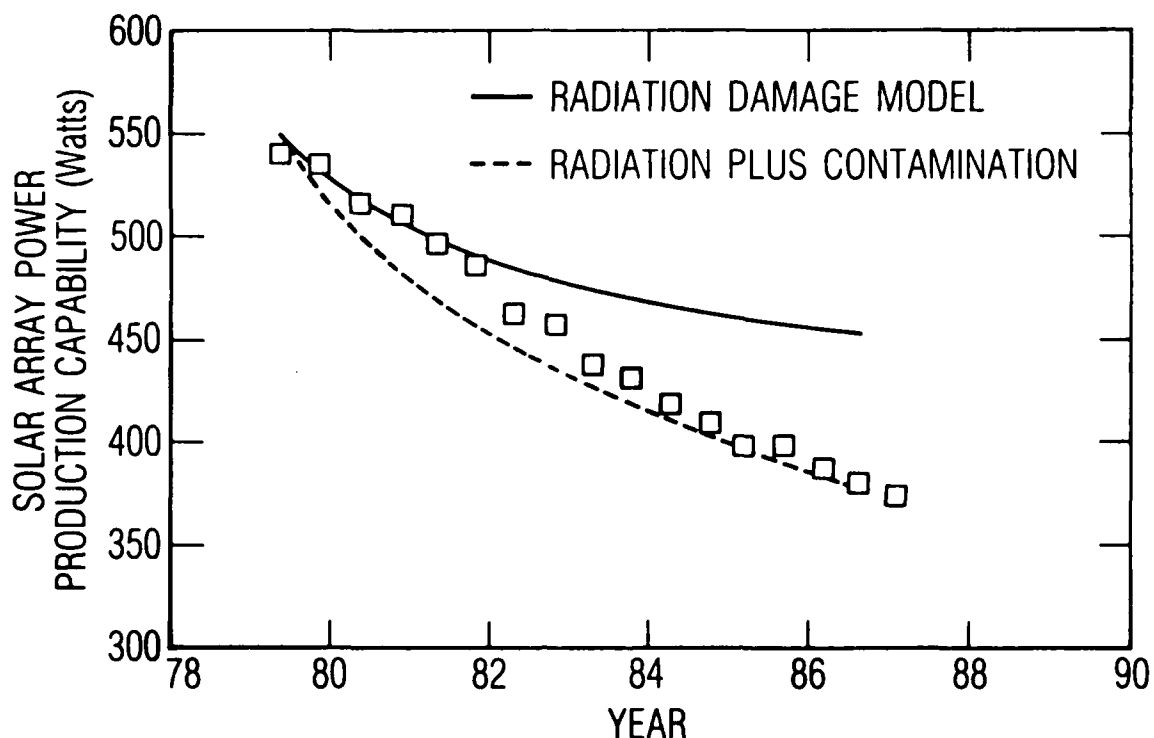


Fig. 12. Predicted and Measured Power Production Capability of NAVSTAR-4 Solar Arrays. The solid line is the radiation damage prediction; the dashed line is the prediction when contamination effects are included.

Grant¹⁰ suggested that the observed darkening did not owe to contamination on the grounds that:

- a. The GPS vehicles are built and assembled using accepted standards of cleanliness in materials and procedures.
- b. The NAVSTAR-5 vehicle underwent a 30-day thermal-vacuum test during which time the "no visual or optical property (α_s) degradation" was observed.
- c. The solar absorptance curve for the fused silica mirror does not exhibit the sort of clear exponential roll off one would expect for a contamination-driven degradation.

Furthermore, a solar array surface runs substantially warmer than the radiator or optical surfaces one normally worries about in contamination control. These arguments are not to be dismissed lightly.

One possible mechanism for explaining the optics degradation on GPS Block I vehicles is radiation-induced darkening of the fused silica used in the OSR or the solar cell cover slips. However, the sort of OSR used in the NAVSTAR-5 calorimeter is known to be quite stable to the near geosynchronous radiation environment. Indeed the material used in these mirrors, Corning 7940 fused silica, is known for its ability to suffer energetic particle radiation without decreasing in transparency (in the visible wavelength range.)¹⁹⁻²⁵ Thus if radiation damage is the cause of the NAVSTAR-5 OSR's darkening, then it must occur by some mechanism not yet identified in the laboratory, or at least at a rate much faster than one would estimate from published data.

Pence and Grant were not in a position to assess the role of photo-chemically-deposited contamination on the results of the NAVSTAR-5 calorimeter when they published their work. To provide such an assessment, we have used a simple geometric model of the GPS vehicle to estimate the contaminant flux onto the GPS solar arrays. Figure 13 shows a two-dimensional representation of the model geometry. Estimates of the vehicle dimensions and the areas and locations of vents were made on the basis of information provided by the prime contractor for the GPS vehicle. Note that no details such as thermal insulation blankets or their seams were included in the model geometry. The term "boom" refers to the supports which connect the solar arrays to the vehicle body.

Contaminant fluxes onto the solar arrays from surface generated and vented contaminants were estimated, taking into account only line-of-sight (LOS) contamination from the surface perpendicular to the solar array. The contaminant flux to each point on the solar array is formally given by

$$F(x_1, y_1) = \int [F_c(A) \cos(\theta) \cos(\phi) / \pi r^2] dA \quad (5)$$

where (x_1, y_1) are the location on the solar array, $F_c(A)$ is the contaminant flux from the differential surface element dA , θ and ϕ are the angles that a vector connecting (x_1, y_1) and dA make with respect to the normals of the two surfaces, and r is the distance between the two surfaces. For the purposes of this calculation, Eq. (5) has been approximated as a finite sum over area

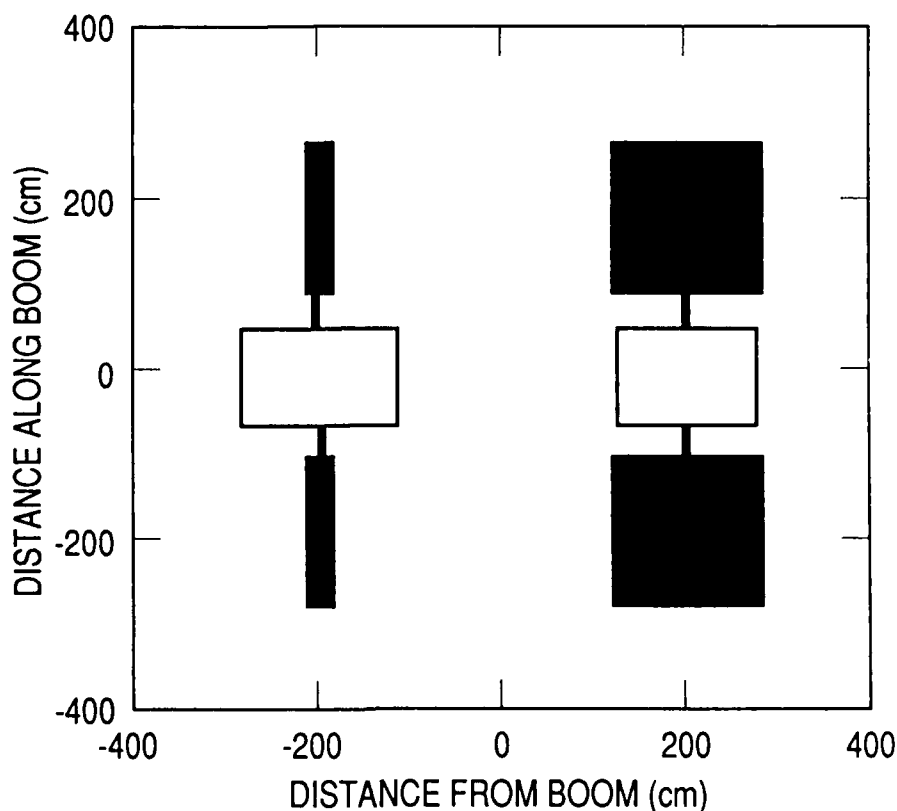


Fig. 13. Simplified Model of the GPS Block I Vehicle Used to Estimate the Contaminant Flux Incident on the Solar Array

elements whose size was chosen such that r^2 is generally large compared to the surface element area, so the approximation used is valid. For contamination by flow from a vent, the sum reduces to a single element. Using the simplified vehicle geometry shown in Fig. 13, one can then compute the average flux onto an element of solar array surface from vent contamination, $\langle F_v \rangle$, and from surface outgassing, $\langle F_s \rangle$. These values appear in Table 5.

To interpret these average fluxes, one must assign some values to the vehicle surface and vent outgassing rates. A generous estimate for the outgassing rate of condensable molecules from a spacecraft surface is $10^{-12} \text{ g cm}^{-2} \text{ sec}^{-2}$. Thus the $\langle F_s \rangle$ values estimated above correspond to approximately $3 \times 10^{-14} \text{ g cm}^{-2} \text{ sec}^{-1}$, or about 100 Å per year (assuming a uniform film with 1 g cm^{-3} density). This is not a sufficient rate to explain the observed optics darkening.

Table 5. Quantities Used in the GPS Solar Array Contamination Model

Quantity	Value	Uncertainty*	Comment
$\langle F_s \rangle^\dagger$	3.4×10^{-2}		See text
$\langle F_v \rangle^{**}$	5.3×10^{-6}		See text
V_r	0.03		See text
Δm	240g	2	See text
ρ	1 g cm^{-3}		Ref. 26 [‡]
τ	590 days	3	Ref. 18, Fig. 2
$\Delta \alpha / \Delta x$	0.005/100 A	5	Ref. 18,27
e	See text	2	Ref. 8

*Uncertainties are multiplicative factors.

[†]In units of outgassing flow from a 1 cm^2 element of surface per cm^2 of collector.

**In units of outgassing flow from the vent per cm^2 of collector.

[‡]In general, organic materials have a specific gravity not much different from 1. See Ref. 26 for numerous examples.

The vent contamination rate can be estimated with the following assumptions:

- The preponderance of the VCM outgassed by the vehicle comes from within the vehicle.
- The source of interior outgassing rate decreases exponentially in time.

Given these assumptions, initial rate of increase in solar absorptance of the NAVSTAR-5 calorimeter is given by

$$\Delta \alpha / \Delta t = \langle F_v \rangle V_r e(\Delta m / \tau) (1 / \rho) (\Delta \alpha / \Delta x) \quad (6)$$

The quantities $\langle F_V \rangle$ and V_r are estimates based on approximate vehicle geometries. There is no basis on which one can assign uncertainties to these quantities. This is not the case for the physical factors in Eq. (6). Values and uncertainties for most of the parameters in Eq. (6) are shown in Table 5.

The laboratory data and kinetic model presented above suggest that the "efficiency of deposition"

$$e^{-1} = a_1 + a_2 F_c \quad (7)$$

where F_c is the arrival rate and a_1 and a_2 are coefficients which depend on the contaminant identity, intensity of illumination, and temperature of the surface. Table 6 shows the values of these coefficients inferred from the laboratory data presented above for two model spacecraft contaminants: dioctyl phthalate (DEHP) and tetramethyltetraphenyl-trisiloxane (DC-704).

The DC-704, 315 K curve lies roughly in the middle of the range of kinetic behavior observed in the laboratory. Furthermore, 315 K is approximately the operating temperature of the GPS solar array. This curve is chosen as the nominal kinetic behavior for modeling the NAVSTAR-5 calorimeter data.

Table 6. Photochemical Deposition Kinetic Parameters

Molecule	Temperature (kelvin)	a_1 (dimensionless)	a_2 (hr/ Angstrom)
DC-704	306	1.56	1.021
DC-704	315	2.69	1.021
DEHP	302	7.7	1.41
DEHP	315	45.8	1.41

Figure 14 shows a comparison between the computed and observed increase in solar absorptance for the NAVSTAR-5 calorimeter. The reader should be aware that this simple computation is not presented as a rigorous contamination model for the GPS Block I vehicle, but rather as an estimate intended to discern whether it is possible that contamination could account for darkening of the magnitude observed on GPS vehicle surfaces. Uncertainties for the physical parameters in the estimate combine to an overall uncertainty in the estimate of about a factor of 7. At the end of this estimate and propagation of errors, the conclusion is, to the extent that the geometric model of GPS vehicles used is valid, that it is possible to account for the magnitude of the increase in solar absorptance of the NAVSTAR-5 calorimeter (and by inference for the degradation in GPS block I solar array performance) by the effect of photochemically deposited contaminants.

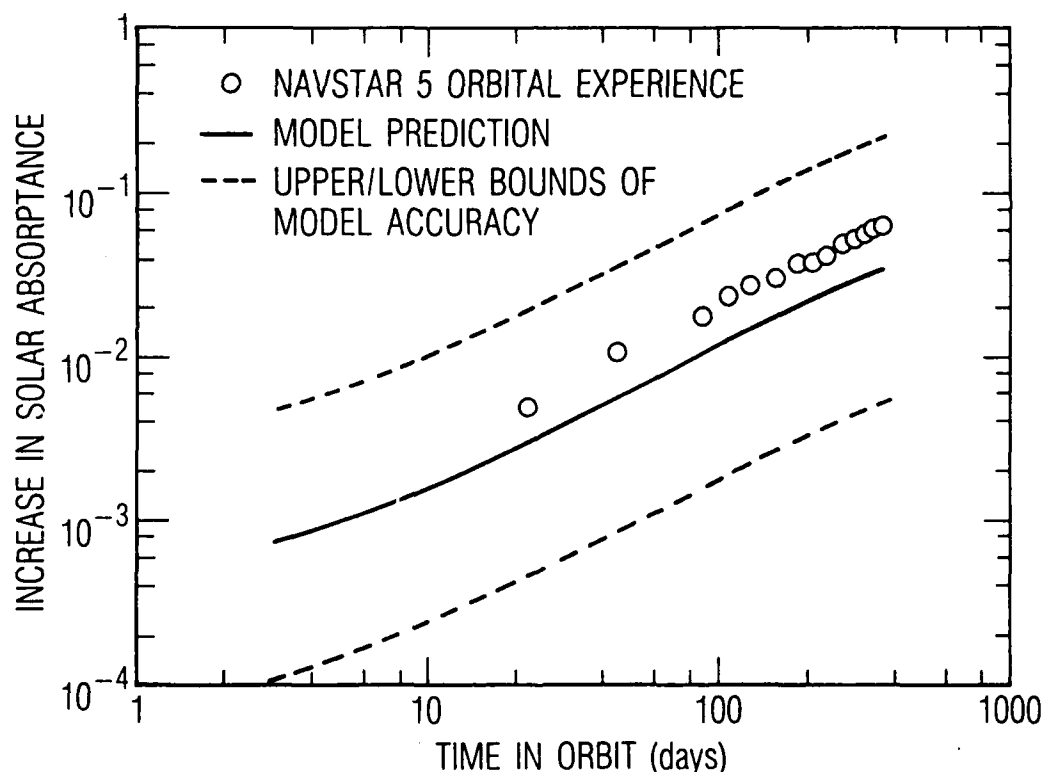


Fig. 14. Estimate of the Increase in Solar Absorptance of a Fused Silica Mirror Mounted on the GPS Solar Array Compared to the NAVSTAR-5 Calorimeter Data. The dashed lines are the estimated range of uncertainty. See text for details.

IV. CONCLUSION

It was previously reported⁶ that a siloxane (Dow Corning 704) was irreversibly deposited onto surfaces by the action of VUV radiation, and that deposition occurred under conditions of arrival rate and surface temperature for which bulk condensation would not occur. New experiments using bis(2,-ethyl,hexyl phthalate), more commonly known as dioctyl phthalate, show the same photochemical behavior as DC-704. Experiments were performed at arrival rates equivalent to 0.2-2 nm/hr (for unit sticking coefficient) which are comparable to those expected to occur at the SDS radiator.⁶

We measured photodeposition rates of 0.01 to 0.1 nm/hr. Isothermal desorption rate measurements showed that the heat of desorption of dioctyl phthalate was 30 kcal/mole, and that the residence time for desorption was approximately 550 s at a surface temperature of about 303 K. The photo-deposition rate was inversely dependent on the surface temperature, exhibiting an apparent activation energy for photodeposition of -13.5 kcal/mole for DC-704 and -26.8 kcal/mole for dioctyl phthalate over a surface temperature range of about 290-310 K. We inferred from the arrival-rate dependence of the deposition rate that the photoabsorption cross sections for DC-704 and dioctyl phthalate were roughly equal to the bulk absorption cross sections of these molecules. The deposition rate exhibited no substantial dependence on irradiation wavelength below 180 nm. Above 200 nm, no deposition was observed. The identity of the substrate affected the deposition rate.

The inverse temperature dependence, arrival rate dependence, inferred photoexcitation cross sections, and substrate dependence of the deposition rate strongly indicate that the reaction rate is controlled by the concentration of transiently adsorbed reactant, and that the mechanism for photo-deposition involves the (unspecified) excitation of an adsorbed contaminant molecule. Calculations based on the bulk absorption cross sections of the molecules show that photoexcitation of incoming gas-phase contaminant molecules cannot account for the deposition rate. A kinetic model, cast in the spirit of the Langmuir model for molecular adsorption, provides a good description of the behavior of the photochemical deposition rate.

Other experiments examined the effect of VUV irradiation on the adhesion of contaminants condensed on cold surfaces. It had been suggested that contaminant films which could potentially accrete on cold surfaces during the orbital transfer period of Inertial Upper Stage (IUS) missions could become photochemically "fixed" to those surfaces by solar irradiation rather than re-evaporating as the spacecraft surfaces warm. Laboratory experiments were performed to test this notion. Although variations in the source material produced variations in the absolute amount of material remaining at high temperature, it was clear that the illumination caused a significant increase in irreversibly deposited mass. For comparison, similar experiments were performed with a model contaminant, dioctyl phthalate. The observation of photochemical fixing was unambiguous in this case.

Further evidence for the effects of contaminant deposition on warm, sunlit surfaces is provided by the observed reduction of the power output of solar arrays on the Global Positioning Satellite (GPS). Conventional radiation degradation models fail to account both for the rate of decrease in array power output and the time dependence of the degradation rate. Calorimeter experiments on the GPS vehicle¹⁰ show a substantial increase in solar absorptance of a fused silica mirror located near the solar array. If this absorptance increase is ascribed to contamination, then one can account quantitatively for the unexpected solar array degradation. Model calculations based on a simplified spacecraft geometry, reasonable estimates of vehicle outgassing, and photochemical deposition kinetics suggest that the level of contamination required for the observed degradation could be incident on the GPS solar array surfaces.

Therefore, it is clear that the role of sunlight is not just to darken or fix previously condensed contaminant films. It can, indeed, promote the irreversible deposition of contaminant films under conditions for which ordinary condensation would not occur. The case is strong that photochemical deposition of contaminant films on sunlit satellite surfaces can have a major, system-level impact on satellite performance and is therefore an important phenomenon which must be considered in designing space vehicles and planning their operations.

REFERENCES

1. J. A. R. Samson, Techniques of Vacuum Ultraviolet Spectroscopy; John Wiley and Sons, New York, (1967), p. 88.
2. C. G. Roffey, Photopolymerization of Surface Coatings, Wiley, New York, (1982).
3. R. Kruger and H. Shapiro, NASA Technical Memorandum 81999, NASA Goddard Space Flight Center, (August, 1980).
4. D. J. Ehrlich and J. Y. Tsao, "A Review of Laser-Microchemical Processing," J. Vac. Sci. Technol. B, vol. 1, no. 4, (1983), pp. 969-984.
5. D. H. Maylotte and A. N. Wright, "Surface Photopolymerization of Tetrafluoroethylene" Faraday Discuss. Chem. Soc. 58, 292-300 (1975).
6. D. F. Hall, T. B. Stewart and R. R. Hayes, "Photo-Enhanced Spacecraft Contamination Deposition," AIAA 20th Thermophysics Conference (June 1985).
7. G. S. Arnold and D. F. Hall, "Contamination of Optical Surfaces," in Space Station Contamination Workshop Proceedings, NASA/MSFC Space Science Laboratory, ed. M. R. Torr, J. F. Spann, and T. W. Moorehead, NASACP-3002 (May 1988) pp. 101-108.
8. T. B. Stewart, G. S. Arnold, D. F. Hall, and H. D. Marten, "Absolute Rates of Vacuum Ultraviolet Photochemical Deposition of Organic Films," J. Phys. Chem. 93, 101-108 (May 1988).
9. H. Y. Tada, J. R. Carter, Jr., B. E. Anspaugh, and R. G. Downing, JPL Solar Cell Radiation Handbook, NASA JPL Pub. 82-69, pp. 3-61-152 (1983).
10. W. R. Pence and T. J. Grant, "Measurements of Thermal Control Coatings on NAVSTAR Global Positioning System Spacecraft," Progress in Astronautics and Aeronautics 83, 234-246 (1982).
11. Diffusion Pump Fluids, Dow Corning, Midland, MI, Bulletin 05-058 (September 1963).
12. P. A. Small, K. W. Small, and P. Cowley, "Vapor Pressure of Some High-Boiling Esters," Trans. Faraday Soc. 44, 810-816 (1948).
13. J. R. McNesby, W. Brown, and J. Ball, in Creation and Detection of the Excited States, ed. A. A. Lamola and M. Dekker, New York (1976). pp. 503-586.

14. J. Kaspar, "Radiometry," in The American Institute of Physics Handbook, ed. D. E. Gray, McGraw-Hill, New York (1972) pp. 6-216-217.
15. B. L. Sowers, M. W. Williams, R. N. Hamm, and E. T. Arakuwa, "Optical Properties of Some Silicone Diffusion-Pump Oils in the Vacuum Ultraviolet - Using a Closed-Cell Technique," J. Appl. Phys. 42, 4252-57 (1971).
16. R. J. Partridge, J. Chem. Phys. 47, No. 10, 47, 4223-4227 (1967).
17. A. L. Fahrenbruch, and R. H. Bube, Fundamentals of Solar Cells, Academic Press, (New York 1983), p. 82.
18. D. F. Hall, "Current Flight Results from the P78-2 (SCATHA) Spacecraft Contamination and Coatings Degradation Experiment," Proceedings of an International Symposium on Spacecraft Materials in Space Environment, European Space Agency, SD-178, Toulouse, France (June 1982).
19. G. W. Arnold, and W. D. Compton, "Radiation Effects in Silica at Low Temperatures," Phys. Rev. 116, (4) 802-11 (1959).
20. M. Antonini, P. Camagni, P. N. Gibson, and A. Mahara, Radiation Effects, vol. 65, (1982) p. 41.
21. D. L. Griscom, "Nature of Defects and Defect Generation in Optical Glasses," SPIE 541, 38-59 (1985).
22. E. J. Friebele, G. H. Sigel, and D. L. Griscom, "Drawing-Defect Centers in a Fused Silica Core Fiber," Appl. Phys. Lett. 28, (9), 516-18 (1976).
23. D. L. Griscom and E. J. Friebele, "Effects of Ionizing Radiation on Amorphous Insulators," Radiation Effects 65, 63-72 (1982).
24. E. J. Friebele, D. L. Griscom, and M. J. Marrone, "The Optical Absorption and Luminescence Bands Near 2 eV in Irradiated and Drawn Synthetic Silica," J. Non-Crys. Solids 71, 133-144 (1985).
25. D. L. Griscom, "Defect Structure of Glasses: Some Outstanding Questions in Regard to Vitreous Silica," J. Non-Crys. Solids 73, 51-77 (1985).
26. R. C. Weast, Handbook of Chemistry and Physics, 50th ed. Chemical Rubber Company, (1970), pp. C-75-542.
27. D. L. Mossman, H. D. Bostic, and J. R. Carlos, "Contamination Induced Degradation of Optical Solar Reflectors in Geosynchronous Orbit," Proceedings of the SPIE, 777, Optical System Contamination: Effects, Measurement, Control, ed. P. Glassford (1987), pp. 2-11.